

Measurement-Based Quantum Metropolis Algorithm

Jonathan E. Moussa

Molecular Sciences Software Institute, Virginia Tech, Blacksburg, Virginia 24060, USA*

We construct a quantum version of a rejection-free classical Metropolis algorithm to prepare quantum thermal states. It samples thermal expectation values without interrupting its quantum Markov chain by driving transitions with observable measurements. Gaussian-filtered quantum phase estimation enables a thermalization timescale proportional to the reciprocal of temperature and the logarithm of biasing error.

We expect universal, efficient, unbiased simulations of quantum thermal states to require quantum algorithms on quantum computers [1]. Following the great successes of classical Markov chain Monte Carlo (MCMC) algorithms in sampling classical thermal states on classical computers [2], a natural progression is to consider quantum MCMC algorithms [3] for this purpose. The simplest approach is to extend an established classical MCMC algorithm such as the Metropolis algorithm [4] to the quantum case.

Two quantum Metropolis algorithms have already been proposed [5, 6], with two shared components and caveats. To prepare a quantum thermal state, $\rho_\beta = e^{-\beta H} / \text{tr}(e^{-\beta H})$, at a temperature β^{-1} , we need some form of access to the energies E_a and stationary states $|\psi_a\rangle$ of its Hamiltonian,

$$H = \sum_a E_a |\psi_a\rangle\langle\psi_a|. \quad (1)$$

Both algorithms use quantum phase estimation (QPE) [7] to access E_a and $|\psi_a\rangle$ and then apply a unitary operation to drive transitions between $|\psi_a\rangle$. QPE uses Hamiltonian simulation time as a resource to reduce biasing errors to a magnitude that is inversely proportional to the maximum simulation time. Measurements of observables other than H collapse ρ_β and break the quantum Markov chain, and ρ_β must be prepared again to repeat such measurements. Passive, unbiased sampling of thermal expectation values is a cornerstone of the classical Metropolis algorithm that its quantum extensions have failed to retain until now.

We construct a quantum Metropolis algorithm based on two revised components that retains the passive, unbiased sampling of thermal expectation values. Gaussian-filtered QPE (GQPE) defines a positive operator-valued measure (POVM) over ω that collapses an input state $|\Psi\rangle$ into

$$|\Psi(\omega)\rangle \propto \exp[-(\omega - H)^2 / (2\gamma)] |\Psi\rangle \quad (2)$$

and utilizes Hamiltonian simulation time more efficiently by reducing the magnitude of biasing errors exponentially in the maximum simulation time. The transitions between $|\psi_a\rangle$ are directly driven by preparation and measurement

of the local stationary states $|\phi_a\rangle$ of a local observable,

$$L = \sum_a \lambda_a |\phi_a\rangle\langle\phi_a| \otimes I. \quad (3)$$

These measurements preserve the quantum Markov chain as ρ_β mixes and subsequent measurements decorrelate.

To avoid the quantum complications of a rejection step [5], we use a rejection-free classical Metropolis algorithm [8] as the foundation for our quantum algorithm. Fig. 1 is the pseudocode of this stochastic algorithm that defines a conditional probability distribution, $M(b|a)$, from input to output state labels. We show that $M(b|a)$ obeys classical detailed balance in Appendix A, which guarantees that it preserves the thermal distribution $\langle\psi_a|\rho_\beta|\psi_a\rangle$ over input state labels. The conventional Metropolis algorithm [4] is recovered when $P(b|a)$ alternates between pairs of states, which causes the repeat-until-success loop to stop within two iterations and avoid protracted stopping times.

The quantum extension of Fig. 1 in Fig. 2 follows from using GQPE for indirect, imprecise energy measurements and a POVM that drives $P(b|a)$ transitions between $|\phi_a\rangle$ instead of $|\psi_a\rangle$. The quantum-extended pseudocode uses kets to denote quantum variables that are naturally passed by reference. Fig. 2 applies a POVM over E and a to $|\Psi\rangle$

```

1:  $a \leftarrow \text{input}$ 
2:  $q \leftarrow 0$ 
3:  $q_{\max} \leftarrow 0$ 
4:  $E \leftarrow E_a$ 
5: repeat
6:    $b \sim P(b|a)$ 
7:    $a \leftarrow b$ 
8:    $q_{\max} \leftarrow \max\{q_{\max}, q\}$ 
9:    $q \leftarrow \exp[\beta(E - E_a)]$ 
10:   $u \sim \mathcal{U}(0, 1)$ 
11: until  $u \leq (q - q_{\max}) / (1 - q_{\max})$ 
12: output  $\leftarrow b$ 

```

FIG. 1: Rejection-free classical Metropolis algorithm [8] driven by sampling from the uniform distribution over $[0, 1]$, $\mathcal{U}(0, 1)$, and a symmetric conditional probability distribution, $P(b|a)$.

```

1:  $|\Psi\rangle \leftarrow \text{input}$ 
2:  $q \leftarrow 0$ 
3:  $q_{\max} \leftarrow 0$ 
4:  $E \sim \text{POVM}(e^{-(E-H)^2/(2\gamma)}(\pi\gamma)^{-1/4}, |\Psi\rangle)$ 
5:  $a \sim \text{POVM}(|\phi_a\rangle\langle\phi_a| \otimes I, |\Psi\rangle)$ 
6: repeat
7:    $(b, c) \sim \text{POVM}(P(c|b)|\phi_c\rangle\langle\phi_b| \otimes I, |\Psi\rangle)$ 
8:    $E_{\text{new}} \sim \text{POVM}(e^{-(E_{\text{new}}-H)^2/(2\gamma)}(\pi\gamma)^{-1/4}, |\Psi\rangle)$ 
9:    $q_{\max} \leftarrow \max\{q_{\max}, q\}$ 
10:   $q \leftarrow \exp[\beta(E - E_{\text{new}} - \beta\gamma/2)]$ 
11:   $u \sim \mathcal{U}(0, 1)$ 
12: until  $u \leq (q - q_{\max})/(1 - q_{\max})$ 
13: output  $\leftarrow (E, a)$ 

```

FIG. 2: Measurement-based quantum extension of Fig. 1 driven by $a \sim \text{POVM}(K_a, |\Psi\rangle)$, which samples from $\langle\Psi|K_a^\dagger K_a|\Psi\rangle$ with $|\Psi\rangle \leftarrow K_a|\Psi\rangle\langle\Psi|K_a^\dagger K_a|\Psi\rangle^{-1/2}$ as a quantum side effect.

that satisfies quantum detailed balance with its $\beta\gamma/2$ bias correction as shown in Appendix A. It is the combination of Gaussian filters and Boltzmann factors that enables the exact compensation of bias caused by energy uncertainty. Unlike the repeat-until-success circuits used for quantum rotation synthesis [9], each loop iteration from Fig. 2 has nontrivial, irreversible effects. Quantum detailed balance guarantees that ρ_β is a stationary state of Fig. 2 but does not exclude other stationary states. When ρ_β is uniquely stationary, the output E and λ_a are unbiased estimators of $\text{tr}(\rho_\beta H)$ and $\text{tr}(\rho_\beta L)$ measured from the input ρ_β .

The idealized quantum algorithm in Fig. 2 is unbiased, but biasing errors are unavoidable in any quantum circuit implementations of GQPE on lines 4 and 8. Such a circuit is shown in Fig. 3 using n ancillary qubits and up to t_{\max} total Hamiltonian simulation time. It is a variation of the standard QPE circuit utilizing qubit-controlled Hermitian conjugation [10] and quantum spectral filtering [11]. The primary source of error is the restriction of the simulation time interval from \mathbb{R} to $(-t_{\max}, t_{\max})$, and other errors are adjusted to be of comparable size or smaller. As shown in Appendix B, the quantum resource requirements are

$$t_{\max} = (\beta/\pi) \log(1/\epsilon), \quad r = \lceil \log_2[(4/\pi) \log(1/\epsilon)] \rceil, \\ n = \lceil \log_2[(2\beta \max_a |E_a|/\pi^2 + 4/\pi) \log(1/\epsilon)] \rceil, \quad (4)$$

to bound the maximum biasing error in each approximate GQPE operation by ϵ . This analysis does not account for other error sources such as noise in logical quantum gates and approximation errors in Hamiltonian simulation that are assumed to be under control and made negligible.

For any H , L , and $P(a|b)$, the distribution of stopping times for the repeat-until-success loop in Fig. 2 will have a fat tail and a divergent mean. We truncate these fat tails by limiting the repeat-until-success loop to a maximum of N iterations, which is yet another source of biasing error. As shown in Appendix B, $N = \lceil 1/\log_2[(1+\epsilon)/(1-\epsilon)] \rceil$ balances this error against the error in Fig. 3 with Eq. (4).

For $\epsilon \ll 1$, the representative example of a single-energy Hamiltonian has a stopping-time distribution with a mean of $10 \log(1/\epsilon)$ iterations and a variance of $24/\epsilon$ [12].

Quantum thermalization using Figs. 2 and 3 occurs on a Hamiltonian simulation timescale set by t_{\max} in Eq. (4) multiplied by the repeat-until-success stopping timescale and the mixing timescale for the quantum Markov chain. Known Hamiltonian simulation algorithms can be used to relate resource estimates in simulation time to lower-level estimates such as a number of Hamiltonian oracle queries [13] or a circuit depth [14]. As in the classical Metropolis algorithm, we should anticipate long mixing timescales in difficult instances that might be reduced by careful design of L and $P(b|a)$. The same considerations might apply to the stopping timescales for the quantum algorithm. In the simpler case of Fig. 1, the stopping timescale is related to the recurrence timescale of $P(b|a)$, which can be limited by restricting each L to a small subsystem in Fig. 2. As a demonstration, we efficiently thermalize a transverse-field Ising model in Fig. 4 by sweeping over spin flips [12].

In conclusion, we have constructed and demonstrated a practical quantum Metropolis algorithm with efficient bias reduction and passive observable sampling. It serves as a foundation for the development of other quantum MCMC algorithms that retain the same benefits alongside further improvements. For example, coherent chain evolution [6] or quantum analogs of cluster updates [15] may accelerate quantum Markov chain mixing for difficult instances.

The Molecular Sciences Software Institute is supported by NSF Grant No. ACI-1547580. J. E. M. thanks Andrew Baczewski and Norm Tubman for useful discussions.

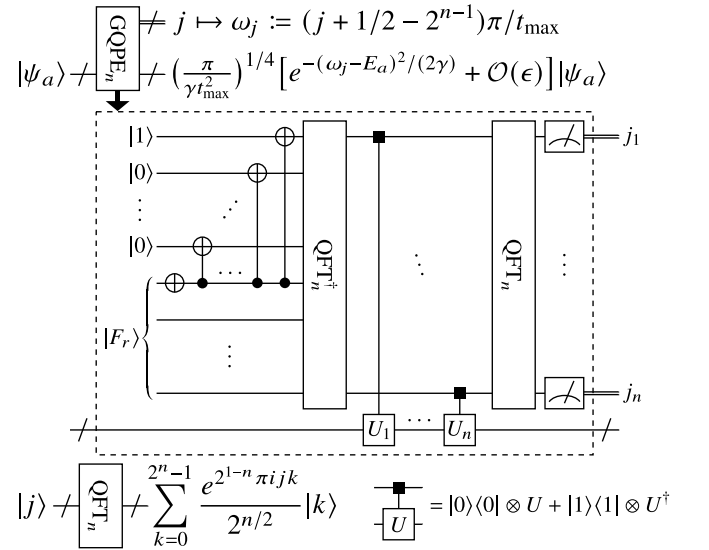


FIG. 3: Approximate quantum circuit implementation of GQPE from lines 4 and 8 of Fig. 2 using n ancillary qubits, the r -qubit resource state $|F_r\rangle$ from Eq. (B3), the standard quantum Fourier transform (QFT) [16], and Hamiltonian time evolution based on $U_j = e^{-iH t_{\max} 2^{-j}}$ operations with a maximum duration of t_{\max} .

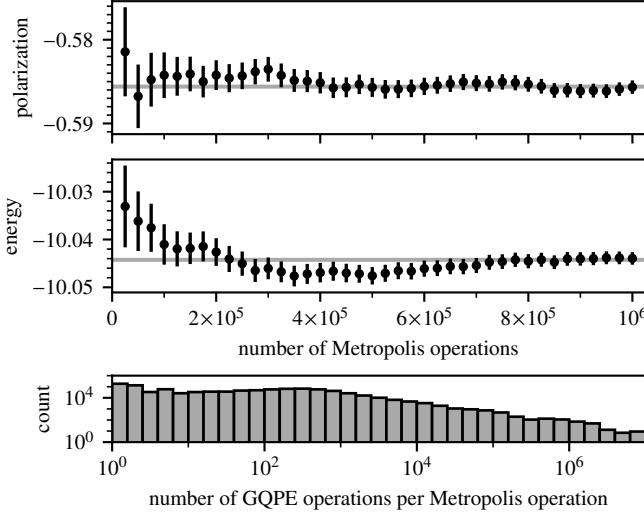


FIG. 4: Stochastic convergence of local polarization, $\text{tr}(\rho_\beta X_i)$, and energy, $\text{tr}(\rho_\beta H)$, to their exact expectation values (gray line) for $H = \sum_{i=1}^8 (X_i - Z_i Z_{1+i \bmod 8})$ at $\beta = 2$, where X_i and Z_i are Pauli operators of the i th qubit. In the i th Metropolis operation, the local POVM is the measurement of $X_{1+(i-1) \bmod 8}$ followed by the application of $Z_{1+(i-1) \bmod 8}$. GQPE operations are based on Fig. 3 and Eq. (4) with $n = 7$, $\epsilon = 10^{-8}$, and error-free U_j .

APPENDIX A: DETAILED BALANCE

We unravel the statistical description $M(b|a)$ of Fig. 1 into all possible iteration numbers and transition paths,

$$\begin{aligned}
 M(b|a) &= \sum_{n=1}^{\infty} \sum_{a_1, \dots, a_{n-1}} \hat{M}(b, a_{n-1}, \dots, a_1|a), \\
 \hat{M}(a_n, \dots, a_1|a_0) &= R_0^n A_0^n \prod_{i=1}^n P(a_i|a_{i-1}), \\
 R_m^n &= \prod_{i=\min\{m,n\}+1}^{\max\{m,n\}-1} (1 - A_m^i), \\
 A_m^n &:= A(a_n, \dots, a_m),
 \end{aligned} \tag{A1}$$

where R_m^n is the probability of reaching a path and A_m^n is the probability of accepting it given a specific sequence of transitions. As in previous work [8], we require that pairs of statistical branches \hat{M} corresponding to each transition path and its reverse independently obey detailed balance,

$$\hat{M}(a_n, \dots, a_1|a_0) p_{a_0} = \hat{M}(a_0, \dots, a_{n-1}|a_n) p_{a_n} \tag{A2}$$

for $p_a = e^{-\beta E_a}$, which is a stricter condition than detailed balance of $M(b|a)$. We can simplify Eq. (A2) further to

$$A_0^n R_0^n p_{a_0} = A_n^0 R_n^0 p_{a_n} \tag{A3}$$

by factoring out path-reversal symmetric $P(b|a)$ terms in \hat{M} , which acts as a constraint on acceptance functions A_m^n .

Subject to this constraint, we achieve the greedy maximum for each acceptance probability with the choice

$$A_m^n = \min\{(R_m^n p_{a_n}) / (R_n^m p_{a_m}), 1\}, \tag{A4}$$

which is correspondingly implemented in Fig. 1.

The quantum version in Fig. 2 is a completely positive trace-preserving map \mathcal{M} of $|\Psi\rangle$ when marginalized over E and a outputs. In a state transition basis, we unravel its description by iteration number and transition paths,

$$\begin{aligned}
 \mathcal{M}(\rho) &= \sum_{a,b,c,d} \mathcal{M}_{ca}^{db} |\psi_c\rangle \langle \psi_a| \rho |\psi_b\rangle \langle \psi_d|, \\
 \mathcal{M}_{ca}^{db} &= \sum_{n=1}^{\infty} \sum_{\substack{a_1, \dots, a_{n-1} \\ b_1, \dots, b_{n-1}}} \hat{\mathcal{M}}_{ca_{n-1} \dots a_1 a}^{db_{n-1} \dots b_1 b}, \\
 \hat{\mathcal{M}}_{a_n \dots a_0}^{b_n \dots b_0} &= \left[\prod_{i=0}^n \mathcal{G}_i \right] \mathcal{R}_0^n(0) A_0^n(0) \prod_{i=1}^n \mathcal{P}_i, \\
 \mathcal{G}_n &:= e^{-(\Omega_n^-)^2/\gamma} \int_{-\infty}^{\infty} \frac{d\omega_n}{\sqrt{\pi\gamma}} e^{-(\omega_n - \Omega_n^+)^2/\gamma}, \\
 \Omega_n^\pm &= (E_{a_n} \pm E_{b_n})/2, \\
 \mathcal{R}_m^n(\Omega) &= \prod_{i=\min\{m,n\}+1}^{\max\{m,n\}-1} [1 - A_m^i(\Omega)], \\
 A_m^n(\Omega) &:= \mathcal{A}(\omega_n, \dots, \omega_{m+\text{sgn}(n-m)}, \omega_m + \Omega), \\
 \mathcal{P}_n &= \sum_{c_n, d_n} P(c_n|d_n) \Theta_{a_n a_{n-1}}^{c_n d_n} \Theta_{b_{n-1} b_n}^{d_n c_n}, \\
 \Theta_{cd}^{ab} &= \langle \psi_c | (|\phi_a\rangle \langle \phi_b| \otimes I) | \psi_d \rangle,
 \end{aligned} \tag{A5}$$

where the reach and acceptance probabilities, $\mathcal{R}_m^n(0)$ and $A_m^n(0)$, now depend on sequences of GQPE measurement outcomes ω_n rather than direct state energies. Similar to the classical case, we guarantee quantum detailed balance [5] with a stricter condition on pairs of branches $\hat{\mathcal{M}}$,

$$\hat{\mathcal{M}}_{a_n \dots a_0}^{b_n \dots b_0} \sqrt{p_{a_0} p_{b_0}} = \hat{\mathcal{M}}_{b_0 \dots b_n}^{a_0 \dots a_n} \sqrt{p_{a_n} p_{b_n}}. \tag{A6}$$

We shift Boltzmann factors $e^{-\beta E}$ from unobserved E_a to measured ω_n using the Gaussian integral identity

$$\begin{aligned}
 \int_{-\infty}^{\infty} d\omega f(\omega) e^{-(\omega - E)^2/\gamma - \beta E} &= e^{-\beta^2 \gamma/4} \\
 \times \int_{-\infty}^{\infty} d\omega f(\omega + \beta\gamma/2) e^{-\beta\omega - (\omega - E)^2/\gamma},
 \end{aligned} \tag{A7}$$

which allows us to factor out the path-reversal symmetric dependence on a_n, b_n, c_n , and d_n from Eq. (A6) to get

$$A_0^n(\frac{\beta\gamma}{2}) \mathcal{R}_0^n(\frac{\beta\gamma}{2}) e^{-\beta\omega_0} = A_n^0(\frac{\beta\gamma}{2}) \mathcal{R}_n^0(\frac{\beta\gamma}{2}) e^{-\beta\omega_n}. \tag{A8}$$

The constraints on acceptance functions in Eqs. (A3) and (A8) are equivalent up to a $\beta\gamma/2$ bias correction.

APPENDIX B: ERROR ANALYSIS

We build a quantum circuit approximation of GQPE by expanding the POVM from Eq. (2) into a measurement of an ancillary continuous quantum variable ω ,

$$|\Psi(\omega)\rangle \otimes |\omega\rangle \propto \int_{-\infty}^{\infty} dt \frac{e^{i\omega t}}{\sqrt{2\pi}} g(t) e^{-iHt} |\Psi\rangle \otimes |\omega\rangle, \quad (B1)$$

$$g(t) = \int_{-\infty}^{\infty} d\omega \frac{e^{-i\omega t}}{\sqrt{2\pi}} \frac{e^{-\omega^2/(2\gamma)}}{(\pi\gamma)^{1/4}},$$

that is prepared with a narrow Gaussian filter over ω , then Fourier transformed into a wide Gaussian filter over t and used as a control of Hamiltonian time evolution duration before its inverse Fourier transform back to ω . With only n ancillary qubits available, we approximate the integrals over continuous quantum variables by finite sums over

$$\omega_j = \omega_{\max} \frac{2j+1-2^n}{2^n}, \quad t_j = t_{\max} \frac{2j+1-2^n}{2^n}, \quad (B2)$$

for $j \in \{0, \dots, 2^n - 1\}$. If these sums are constrained by $\omega_{\max} t_{\max} = 2^{n-1}\pi$, then they can be implemented with the standard QFT as shown in Fig. 3. We group excess phase rotations with an initial ancillary state limited to r qubits,

$$|F_r\rangle \propto \sum_{j=0}^{2^r-1} e^{-i(1-2^{-n})\bar{\omega}_j t_{\max} - \bar{\omega}_j^2/(2\gamma)} |j\rangle \quad (B3)$$

for $\bar{\omega}_j = \omega_{j+2^{n-1}-2^{r-1}}$. The preparation of $|F_r\rangle$ is likely to require $\mathcal{O}(2^r)$ gates [17], thus we must carefully choose r alongside n and t_{\max} to balance cost and accuracy.

Detailed balance of our quantum Metropolis algorithm is robust to this GQPE discretization because the identity in Eq. (A7) is also satisfied by infinite summations,

$$\sum_{j \in \mathbb{Z}} f(\omega_j) e^{-(\omega_j - E)^2/\gamma - \beta E} = e^{-\beta^2 \gamma/4} \times \sum_{j \in \mathbb{Z}} f(\omega_j + \beta\gamma/2) e^{-\beta\omega_j - (\omega_j - E)^2/\gamma}, \quad (B4)$$

if $\beta\gamma t_{\max}/(2\pi)$ is an integer. This constrains the choice of γ , and we choose $\gamma = 2\pi/(\beta t_{\max})$ to minimize the effects of the bias correction in Fig. 2 in that E_{new} only needs to be one grid point lower than E on the finite energy grid to terminate the repeat-until-success loop with certainty.

Since the discretization of POVM outcomes in Eq. (2) does not interfere with detailed balance, the biasing errors are distortions of its Gaussian form in Fig. 3,

$$\tilde{G}(\omega) = \sum_{j=0}^{2^n-1} \sum_{k=0}^{2^r-1} \frac{e^{i(\omega - \bar{\omega}_k)t_j - \bar{\omega}_k^2/(2\gamma)}}{2^n}, \quad (B5)$$

over the domain $|\omega| \leq \Omega_{\max} = (1 - 2^{-n})\omega_{\max} + E_{\max}$ with $E_{\max} = \max_a |E_a|$. We quantify the errors in this Fourier

approximation by its maximum deviation, which depends on four dimensionless parameters $-\beta E_{\max}$, β/t_{\max} , r , and n – in an empirical bound based on error asymptotics,

$$\min_{\delta \in \mathbb{C}} \max_{\omega \in [-\Omega_{\max}, \Omega_{\max}]} |e^{-\omega^2/(2\gamma)} - (1 + \delta)\tilde{G}(\omega)| \leq \epsilon, \quad (B6)$$

$$\epsilon = \exp[-\min\{\pi t_{\max}/\beta, 2^{2(r-1)}\pi\beta/(4t_{\max}), (2^{n-1} - E_{\max}t_{\max}/\pi)^2\pi\beta/(4t_{\max})\}],$$

contingent on $E_{\max} \leq \omega_{\max}$ [12]. The resource estimate in Eq. (4) minimizes t_{\max} , r , and n for a given ϵ .

The biasing error in each approximate GQPE operation accumulates over the iterations of the repeat-until-success loop in Fig. 2 and between successive instances of Fig. 2 in a thermalizing quantum Markov chain. For every loop iteration, the Gaussian weights from \mathcal{G}_n in Eq. (A5) incur an error bounded by $2\epsilon/(1 - \epsilon)$. When compounded over N iterations using the triangle inequality, this error bound grows to $[(1 + \epsilon)/(1 - \epsilon)]^N - 1$. It achieves saturation at $N = \lceil 1/\log_2[(1 + \epsilon)/(1 - \epsilon)] \rceil$, and we then halt the loop without an increase in its boundable error. While a more detailed error analysis is beyond the scope of this Letter, Markov chains dissipate the effects of past biasing errors, and their stationary states only accumulate biasing errors over the mixing timescale rather than the chain length.

* Electronic address: godotalgorithm@gmail.com

- [1] R. P. Feynman, *Int. J. Theor. Phys.* **21**, 467 (1982).
- [2] D. P. Landau and K. Binder, *A Guide to Monte Carlo Simulations in Statistical Physics*, (Cambridge University Press, Cambridge, 2015).
- [3] B. M. Terhal and D. P. DiVincenzo, *Phys. Rev. A* **61**, 022301 (2000).
- [4] N. Metropolis, A. W. Rosenbluth, M. N. Rosenbluth, A. H. Teller, and E. Teller, *J. Chem. Phys.* **21**, 1087 (1953).
- [5] K. Temme, T. J. Osborne, K. G. Vollbrecht, D. Poulin, and F. Verstraete, *Nature* **471**, 87 (2011).
- [6] M.-H. Yung and A. Aspuru-Guzik, *Proc. Nat. Acad. Sci. USA* **109**, 754 (2012).
- [7] D. S. Abrams and S. Lloyd, *Phys. Rev. Lett.* **83**, 5162 (1999).
- [8] A. Mira, *Metron* **59**, 231 (2001).
- [9] A. Paetznick and K. M. Svore, *Quantum Inf. Comput.* **14**, 1277 (2014).
- [10] R. Babbush, C. Gidney, D. W. Berry, N. Wiebe, J. McClean, A. Paler, A. Fowler, and H. Neven, *Phys. Rev. X* **8**, 041015 (2018).
- [11] F. Fillion-Gourdeau, S. MacLean, and R. Laflamme, *Phys. Rev. A* **95**, 042331 (2017).
- [12] The software and data for all numerical results are available at <https://github.com/godotalgorithm/quantum-metropolis>.
- [13] G. H. Low and I. L. Chuang, *Quantum* **3**, 163 (2019).
- [14] A. M. Childs and Y. Su, *Phys. Rev. Lett.* **123**, 050503 (2019).
- [15] R. H. Swendsen and J.-S. Wang, *Phys. Rev. Lett.* **58**, 86 (1987).
- [16] D. Coppersmith, [arXiv:quant-ph/0201067](https://arxiv.org/abs/quant-ph/0201067).
- [17] V. V. Shende, S. S. Bullock, and I. L. Markov, *IEEE Trans. Comput.-Aided Des. Integr. Circuits Syst.* **25**, 1000 (2006).